ACS OMEGA

http://pubs.acs.org/journal/acsodf

Article

Influence of Provenance and the Sedimentary Environment on the Formation of High-Quality Source Rocks in the Paleocene Lishui Sag, China

Luyao Zhang, Xiang Zeng,* Weilin Zhu, Lingcong Yuan, and Jingong Cai*

Cite This: *ACS Omega* 2022, 7, 5791−5803

Read Online

ACCESS | Metrics & More | Article Recommendations | Supporting Information

ABSTRACT: Organic matter (OM) is the material basis for hydrocarbon generation. Its type and abundance determine the hydrocarbon generation ability of source rocks, which is closely related to the provenance and sedimentary environment of source rocks. The tectonic backgrounds of the eastern and western subsags (ESS and WSS) of the Lishui Sag in the East China Sea Shelf Basin are significantly different and their influence on the OM in the source rocks is worthy of attention. This paper comprehensively analyzes the provenance and environmental characteristics and their influence on the features of the OM of Paleocene source rocks in the ESS and WSS. The study finds that the source rocks in the ESS have multiple sources. During the deposition period, as the salinity and paleoproductivity of the water column increased, the proportion of OM in the autochthonous components of the water column continued to increase, but the overall water column was in an oxidizing environment, resulting in a generally low abundance of OM. The provenance of the source rocks in the WSS was relatively simple and terrestrial. Also, the sedimentary environment had little effect on the type of OM. However, the whole water column of the WSS was in an anoxic environment, so the OM was better preserved, resulting in a higher abundance. Due to the influence of provenance and the sedimentary environment in different areas of the sag, the characteristics of OM in the source rocks are different, so relevant exploration strategies need to be adopted in actual exploration.

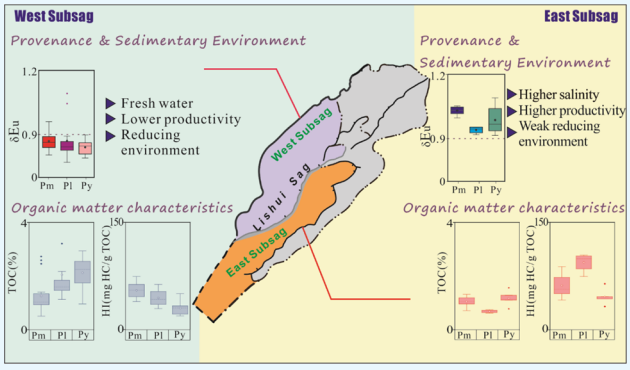

1. INTRODUCTION

Argillaceous source rocks are composed of minerals and organic matter (OM). In particular, OM originating from allochthonous and autochthonous sources is the material basis for hydrocarbon generation.[1,2] The physical and chemical properties of these OM are obviously different, which also dominate the hydrocarbon generation ability of source rocks.[3,4] The type and enrichment of OM in the water column are affected by various factors such as input, preservation, and dilution of OM.[5] During the sedimentation period, the content of OM input from terrigenous sources is usually higher in the proximal and shallow water environment. At the same time, terrigenous detrital components can also dilute the autochthonous OM in the water column and as the sedimentation environment becomes deeper and distal, the provenance of OM gradually changes from terrestrial to aquatic.[3] The changes of redox conditions and salinity in water largely influence the enrichment and deposition of OM. Previous studies have found that the reduction conditions at the bottom of the water column and certain salinity are favored for the preservation of OM.[5−8] In addition, the increase of water salinity is accompanied by changes in OM types and geochemical characteristics.[9,10] Water productivity also affects the enrichment of OM in source rocks. Higher water paleoproductivity reflects a large amount of autochthonous OM.[11] Moreover, different tectonic backgrounds often indicate extreme variation in sedimentary environments,[12,13] which will lead to differences in the enrichment of OM. Therefore, to clarify the characteristics and abundance of OM in sedimentary rocks, investigations of source areas and their sedimentary environment, paleoproductivity, and tectonic background should be highlighted.

Here, the Lishui Sag in the East China Sea Basin was chosen as the study area to investigate the interplay between these environmental factors and the characteristics of buried OM. As an intensively studied area, previous research has investigated the hydrocarbon generation parameters and hydrocarbon

Received: October 14, 2021
Accepted: February 3, 2022
Published: February 13, 2022

https://doi.org/10.1021/acsomega.1c05764
ACS Omega 2022, 7, 5791−5803

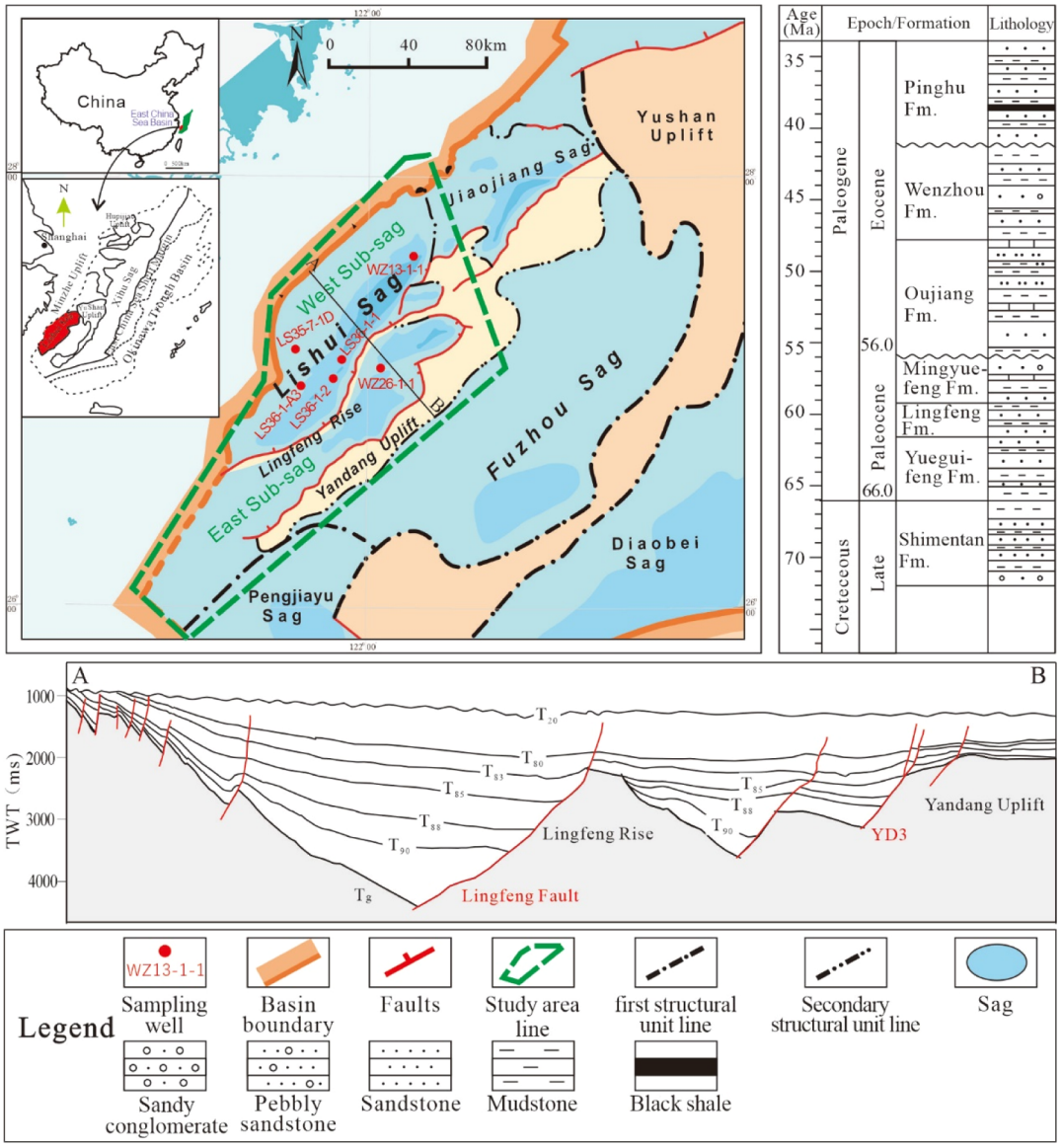

Figure 1. Tectonic sketch and comprehensive stratigraphic column of the Lishui Sag.

generation capacity of this sag.[14] Thick dark mudrocks of the Paleocene Yueguifeng Formation (Py), Lingfeng Formation (Pl), and Mingyuefeng Formation (Pm) have been identified as the main source rocks.[15,16] However, during the Paleocene depositional period, there were large differences in the tectonic backgrounds of the eastern and western subsags (ESS and WSS).[17] In addition, previous studies on the sandstone in this area found that the mineral composition of the sandstone in two subsags (east and west) is obviously different,[18] which indicates that the two areas may have different provenances. However, whether changes in the sedimentary environment and provenance affect the formation and hydrocarbon generation of source rocks in the Lishui Sag remains unclear. This paper aims to identify differences in provenance between the ESS and WSS and the evolutionary history of the sedimentary environment in different periods. Furthermore, the impact of the difference in provenance and sedimentation on the abundance and type of OM in source rocks is evaluated, thereby providing a more complete explanation for the difference between the formation and hydrocarbon generation of source rocks in the ESS and WSS.

2. GEOLOGICAL SETTINGS

The Lishui Sag is located in the southwestern part of the western depression belt of the East China Sea Shelf Basin, and it has a total area of approximately 1.46×10^4 km^2. The sag extends in the NE−SW direction. It is separated from the Fuzhou Sag by the Yandang Uplift in the southeast, the Jiaojiang Sag in the north, and the Minzhe Uplift in the west. The whole sag is a single-faulted half-graben rift, which is a faulted basin dominated by Paleocene−Eocene formations developed on Late Cretaceous basement. The interior of the sag is split by the Lingfeng Rise, which can be further divided into the ESS and WSS (Figure 1). Their areas are approximately 4800 and 9800 km^2, respectively. The tectonic evolution of the Lishui Sag can be divided into four stages: rift, depression, erosion, and overall subsidence. There are obvious differences in the tectonic patterns between the WSS and ESS: the structural framework of the western slope of the WSS was relatively stable, so the Lingfeng fault penetrated rapidly at the early stage of the rift and became the main basin-controlling fault. The ESS's main faults were divided into four relatively

https://doi.org/10.1021/acsomega.1c05764
ACS Omega 2022, 7, 5791−5803

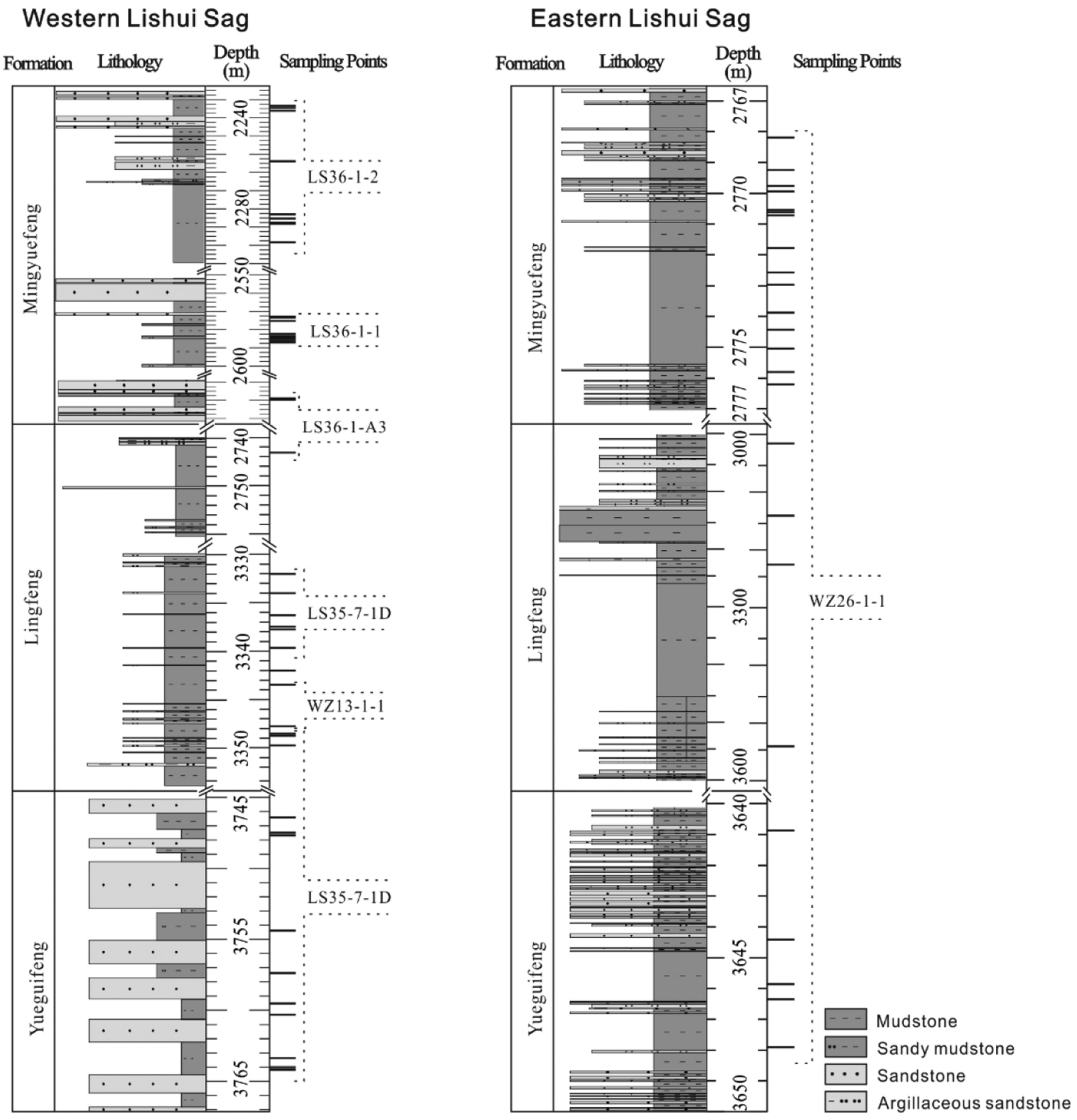

Figure 2. Distribution of samples in each formation.

independent small-scale faults due to the lack of paleo weak zone (Figure 1).[19] Throughout the evolution of the Paleocene, the ESS was closer to the open sea, whereas the WSS was closer to the Minzhe Uplift.[19]

During the Paleocene deposition period, the Lishui Sag experienced a transformation from lake to sea and the water depth increased. The ESS was greatly influenced by the changes of the sea level, whereas the WSS was relatively less affected due to the obstruction of the Lingfeng Rise. The Lishui Sag developed abundant mudstone during the deposition of the Paleocene Yueguifeng–Mingyuefeng Formation (Figure 1). The mudstones deposited in these three sets of strata are the most important source rock intervals in the sag.[15,20]

3. METHODS

In this study, 69 core samples from all 6 wells, including LS35-7-1D, WZ13-1-1, LS36-1A3, LS36-1-1, and LS36-1-2 in the WSS and WZ26-1-1 in the ESS were selected for research, of which 27 blocks were sampled from the ESS and 42 blocks were sampled from the WSS (Figure 2). The sampling depth range was 2233–3765 m. These samples cover the three main source rock strata of the ESS and WSS. After pretreatment, we performed thin-section observations, geochemical element measurements, and pyrolysis analysis.

3.1. Thin-Section Observations. A comprehensive petrographical examination for 50 rock thin sections was performed using an Olympus BX51 microscope. These thin sections were analyzed under optical plane-polarized and fluorescent light at magnifications ranging from 50× to 500×.

3.2. Elemental Measurements. This study conducted elemental analysis on 68 samples. For major and trace element concentrations, a two-step acid digestion method (first with HNO_3 and second with mixtures of HNO_3, HF, and $HClO_4$) was used prior to determination to retain any volatile elements of the studied samples in solution. The resulting solutions were analyzed by inductively coupled plasma atomic emission spectrometry (Thermo ICP-IRIS Intrepid II, Thermo Fisher, Shanghai, China) for major element concentrations and by inductively coupled plasma mass spectrometry (Thermo X-Series, Thermo Fisher, Shanghai, China) for trace element concentrations.

3.3. Pyrolysis. A total of 62 samples were selected for pyrolysis analysis. The samples were powdered to 100 mesh

https://doi.org/10.1021/acsomega.1c05764
ACS Omega 2022, 7, 5791−5803

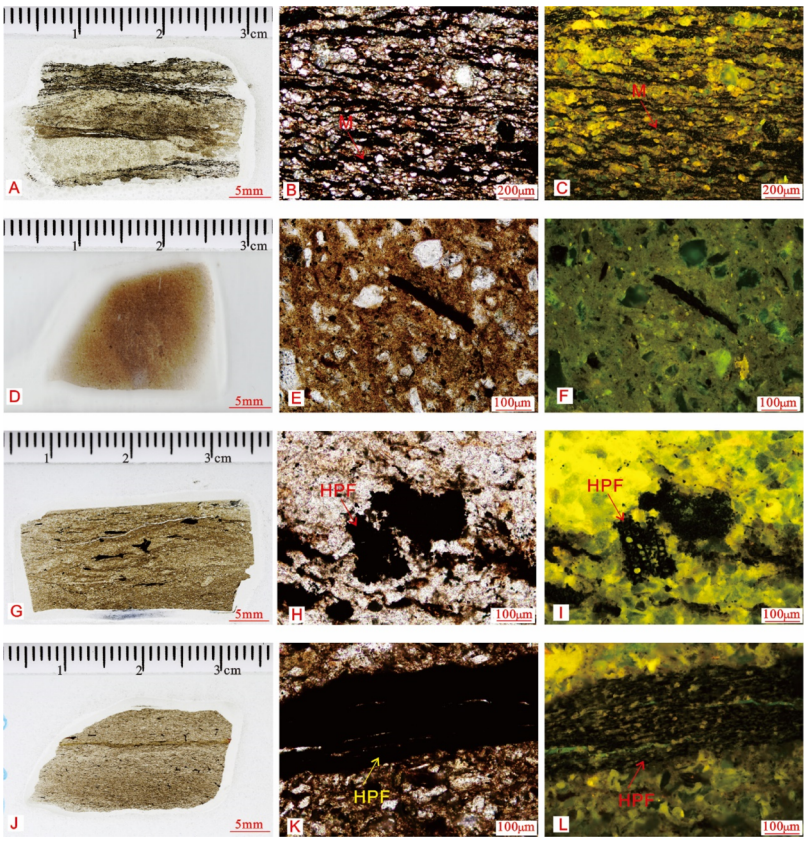

Figure 3. Petrological characteristics. (A) Carbonaceous laminae are visible in the scans of thin sections (ESS, WZ26-1-1, 3640.1 m). (B) Carbonaceous laminae are approximately parallel on the substrate. (C) Carbonaceous laminae are approximately parallel on the substrate (under fluorescent light). (D) Mudstones with massive structure (WSS, LS35-7-1D, 3336.2 m). (E) Carbonaceous fragments preserved in the mud matrix. (F) Carbonaceous fragments preserved in the mud matrix under fluorescence light. (G) Carbonaceous chips are visible on the substrate (WSS, LS36-1-1, 2587.7 m). (H) Morphology of higher plant fragment (HPF) under the translucent lens. (I) Cell structure remaining on the surface of the HPF is visible under fluorescence. (J) OM fragments distributed on the rock surface are visible under the microscope (WSS, LS35-7-1D, 3759.5 m). (K) Shape of HPF under the translucent lens. (L) Residual cell structure on the surface of HPF under fluorescence.

Table 1. Pyrolysis Characteristics of Wells in the Lishui Sag

wells	TOC (%)	HI (mg CO_2/g org. C)	OI (mg CO_2/g org. C)	PC (%)	RC (%)
LS35-7-1D	0.97 − 2.94 / 1.93	19 − 61 / 37	6 − 31 / 14	0.04 − 0.12 / 0.08	0.92 − 2.82 / 1.69
LS36-1-1	0.89 − 2.73 / 1.34	45 − 58 / 51	24 − 61 / 42	0.06 − 0.21 / 0.10	0.83 − 2.52 / 1.24
LS36-1-2	0.52 − 1.07 / 0.92	39 − 70 / 54	27 − 96 / 47	0.06 − 0.08 / 0.07	0.46 − 1.00 / 0.85
LS36-1-A3	2.46 − 3.21 / 2.75	53 − 74 / 66	9 − 14 / 11	0.21 − 0.23 / 0.22	2.25 − 2.36 / 2.31
WZ26-1-1	0.63 − 1.57 / 1.02	32 − 104 / 64	11 − 106 / 38	0.03 − 0.12 / 0.08	0.54 − 1.49 / 0.94

after surface cleaning and pyrolyzed using a Rock-Eval 6 instrument (RE6, Vinci Technologies, Nanterre, France). A series of successive steps were performed. First, 50 mg of each sample was subjected to a temperature of 300 °C, and a hydrocarbon (peak S1, mg/g of rock) was qualified. Second, programmed pyrolysis was performed at temperatures increasing from 300 to 650 °C to qualify the potential hydrocarbons (peak S2, mg/g of rock). Simultaneously, oxygenated products, including CO and CO_2, were measured. These products were referred to as peak S3 (mg CO_2/g of rock) at temperatures between 300 and 390 °C, and residual carbon (RC) at 600 °C [which was referred to as peak S4 (mg CO_2/g of rock)] was recorded. A number of parameters, including TOC, hydrogen index (HI), oxygen index (OI), potential carbon (PC), and RC were assessed at S1−S4. The value of T_{max} corresponds to the temperature at the maximum S2.

4. RESULTS

4.1. Petrological Characteristics. Observations of thin sections show that the source rocks in the Lishui Sag generally contain relatively abundant clastic particles (feldspar, quartz, and lithic particles). The sizes of these particles are generally less than 63 μm, and they are well sorted and evenly

https://doi.org/10.1021/acsomega.1c05764
ACS Omega 2022, 7, 5791−5803

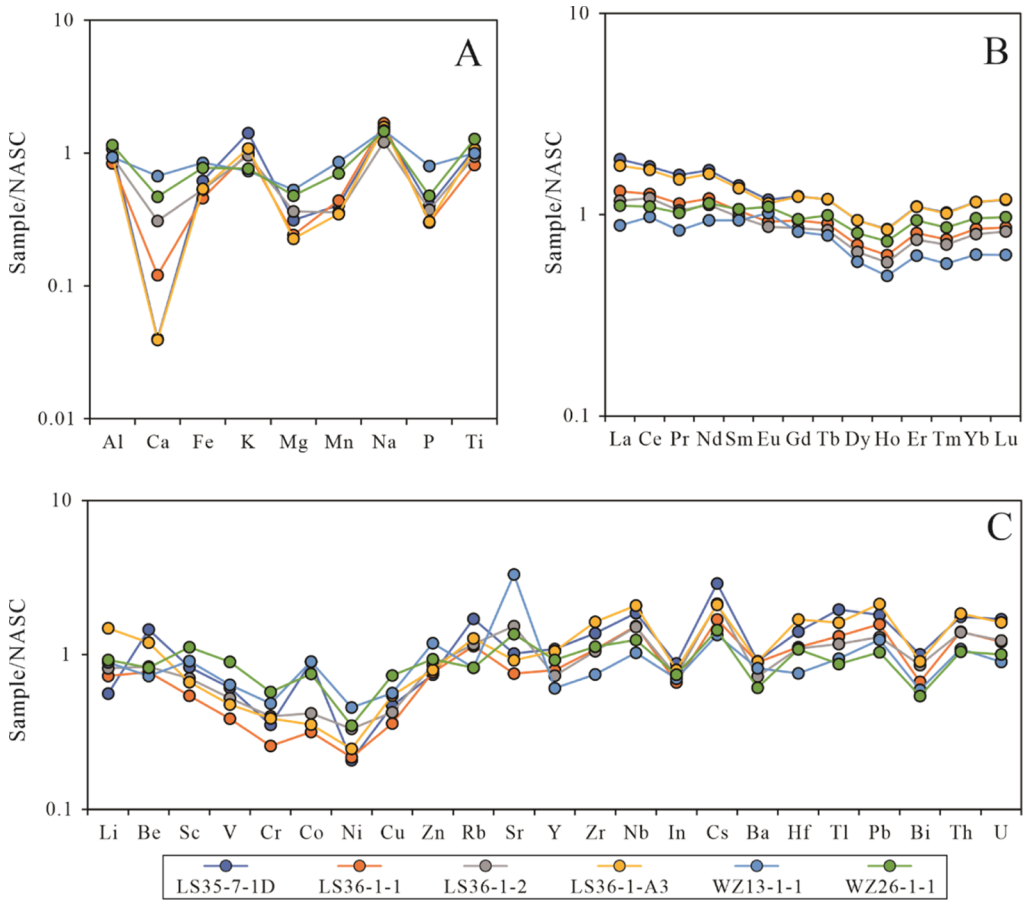

Figure 4. Characteristics of the main and trace elements of each well in the Lishui Sag. (A) NASC-normalized major element diagrams. (B) NASC-normalized REE patterns. (C) NASC-normalized trace element diagrams.

distributed in the mud matrix (Figure 3B,E,H,K). The source rocks in the study area generally have massive and laminar structures. The mudstone with laminar structures is mainly composed of two kinds of laminae: clay-rich laminae and OM-rich laminae (Figure 3B). The massive mudstone shows a relatively homogeneous microstructure and large amounts of detrital minerals distributed in the clay matrix dispersively (Figure 3E,H,K).

The OMs in the rock have many morphologies and some are preserved in the form of carbonaceous laminae that are approximately parallel to each other (Figure 3A−C). This type of OM is generally closely related to the growth of microbial mats. Some OMs are preserved in the form of fragments (Figure 3D−L), and the internal morphology cannot be observed under an optical lens (Figure 3E,H,K). However, under fluorescent light, the residual cell structure on the surface of the OM is visible (Figure 3F,I,L), which indicates that this OM originated from the tissue fragments of terrestrial plants.

In general, the OM in rocks includes both autochthonous OM in the water column and OM input from terrigenous sources, which are preserved in different forms.

4.2. Pyrolysis Results. The pyrolysis analysis of the samples from 5 wells in this study shows that the abundance of OM in each well is in the range of 0.52−3.21% (Table 1) and is 1.36% on average. The HI values are 19−104 mg/g, with an average of 28 mg/g. The OI values are 6−106 mg/g, and the average is 46 mg/g. From the perspective of pyrolysis parameters, the abundance of OM in the source rocks in the Lishui Sag is not high, and the type of OM is mainly type III, which means that the source rock quality is average. The PC values of the rocks range from 0.03 to 0.23%, with an average of 0.9%, and the RC values range from 0.46 to 5.78%, with an average of 1.34%.

4.3. Geochemical Elemental Analysis Results. The source rock samples in the Lishui Sag are standardized by the elemental values of the North American Shale Composite (NASC) to analyze the characteristics of major and trace elements. The major element characteristics show that (Figure 4A) the Al values of the source rock samples are relatively close, and the average values of each well after standardization are in the range of 0.8−1.2, with little difference. The samples generally show Ca, Mg, Mn, and P losses. Among them, the source rocks of well WZ13-1-1 in the ESS have relatively low Ca and P losses. The standardized average values are 0.7 and 0.8, respectively. The loss of Ca and P in other wells is generally higher. In addition, the values of K, Na, and Ti are similar to the NASC values and have little fluctuation.

The rare-earth elements (REEs) of source rock samples from wells in the Lishui Sag are quite different (Figure 4B). The total contents of REEs (ΣREE) in the Paleocene source rock samples are 99.5−374.7 ppm, with an average of 204.7 ppm. After standardization to the NASC, the REE characteristics of source rocks present a left dip (Figure 4B), and the variation range of δEu is 0.76−1.09, with an average of 0.86, showing the characteristics of anomalous negative Eu values.

The trace element values of each well also show obvious variation. Sr fluctuates greatly in the NASC standardized trace

https://doi.org/10.1021/acsomega.1c05764
ACS Omega 2022, 7, 5791−5803

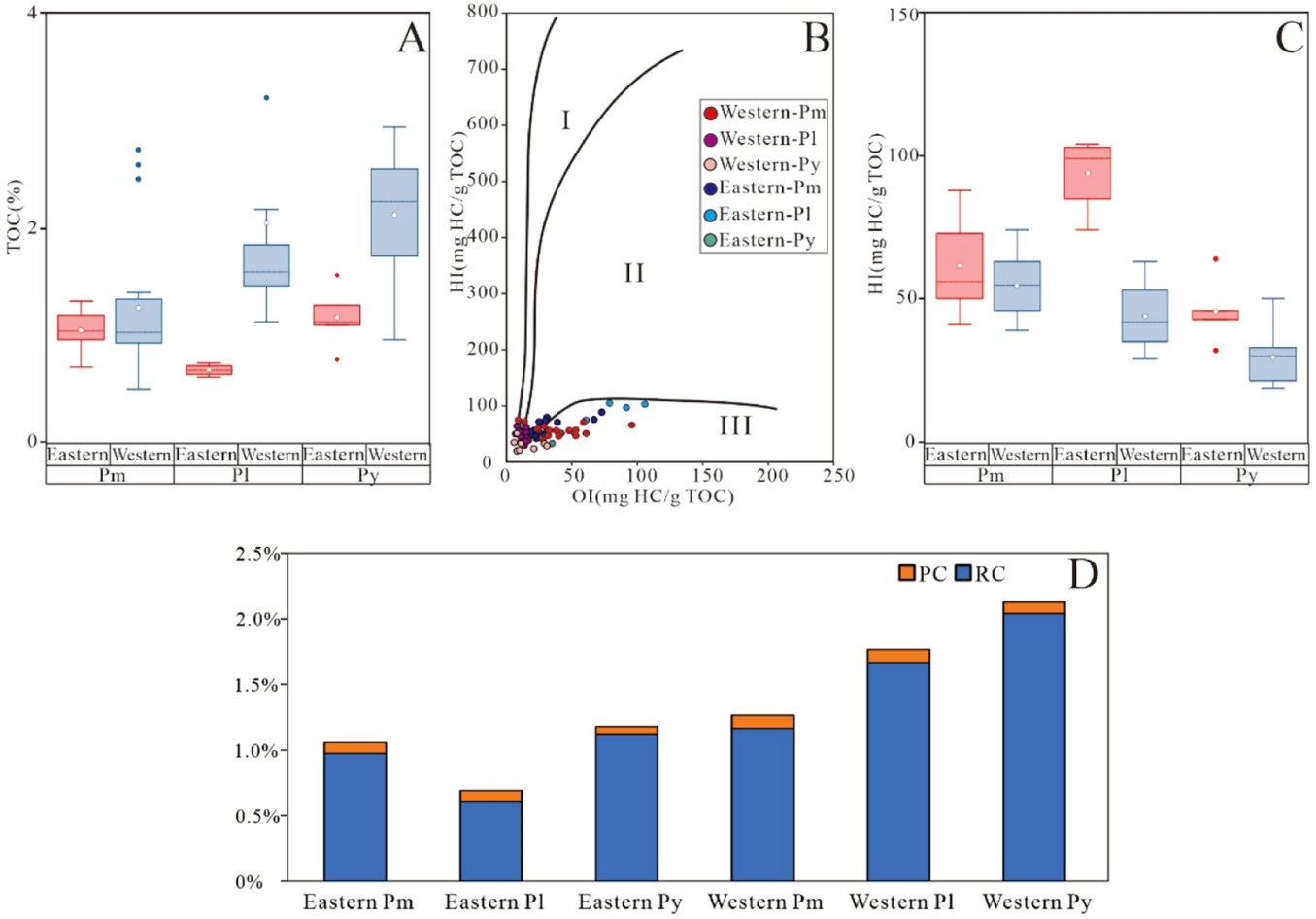

Figure 5. Organic features of each member of the ESS and WSS. (A) TOC characteristics. (B) Kerogen types of source rocks. (C) HI characteristics. (D) PC and RC characteristics.

Table 2. Pyrolysis Characteristics of Formations in the Lishui Sag

formation	TOC (%)	HI (mg CO_2/g org. C)	OI (mg CO_2/g org. C)	PC (%)	RC (%)
Western Pm	0.52 − 2.73 / 1.27	39 − 74 / 55	9 − 96 / 41	0.05 − 0.12 / 0.08	0.67 − 1.25 / 0.97
Western Pl	1.14 − 3.21 / 1.77	29 − 63 / 44	7 − 17 / 13	0.09 − 0.09 / 0.09	0.54 − 0.67 / 0.6
Western Py	0.97 − 2.94 / 2.01	19 − 50 / 29	6 − 31 / 16	0.05 − 0.12 / 0.09	0.92 − 2.82 / 2.04
Eastern Pm	0.81 − 1.33 / 1.06	41 − 88 / 62	19 − 73 / 32	0.05 − 0.12 / 0.08	0.67 − 1.25 / 0.97
Eastern Pl	0.63 − 0.76 / 0.69	74 − 104 / 94	61 − 106 / 85	0.09 − 0.09 / 0.09	0.54 − 0.67 / 0.60
Eastern Py	0.79 − 1.57 / 1.18	32 − 64 / 46	11 − 35 / 18	0.03 − 0.09 / 0.06	0.76 − 1.49 / 1.12

element spider graph (Figure 4C), and the w(Sr) values vary from 119.5 to 725.1 ppm. The fluctuation range of Ba is very small, and the w(Ba) values in the source rock samples of each well vary from 222.2 to 757.6 ppm. The U values are similar to those of the NASC but have a large variation, and the range of $w(U)$ values is 2.0−7.5 ppm.

5. DISCUSSION

5.1. Abundance and Characteristics of the OM Type in Source Rocks. The hydrocarbon generation capacity of source rocks is controlled by the source and evolution of OM. At present, a large number of studies have been conducted on the maturity of source rocks in the Lishui Sag and have determined that the maturity of the source rocks in the ESS and WSS are almost all in the mature stage, and there is no obvious difference between the formations,[15,16] which indicates that the evolution of the source rocks in the entire sag is at the same stage. Then, the quality of the source rocks is mainly affected by the abundance and type of OM. In this study, TOC and HI values of pyrolysis analysis results are used to analyze

https://doi.org/10.1021/acsomega.1c05764
ACS Omega 2022, 7, 5791−5803

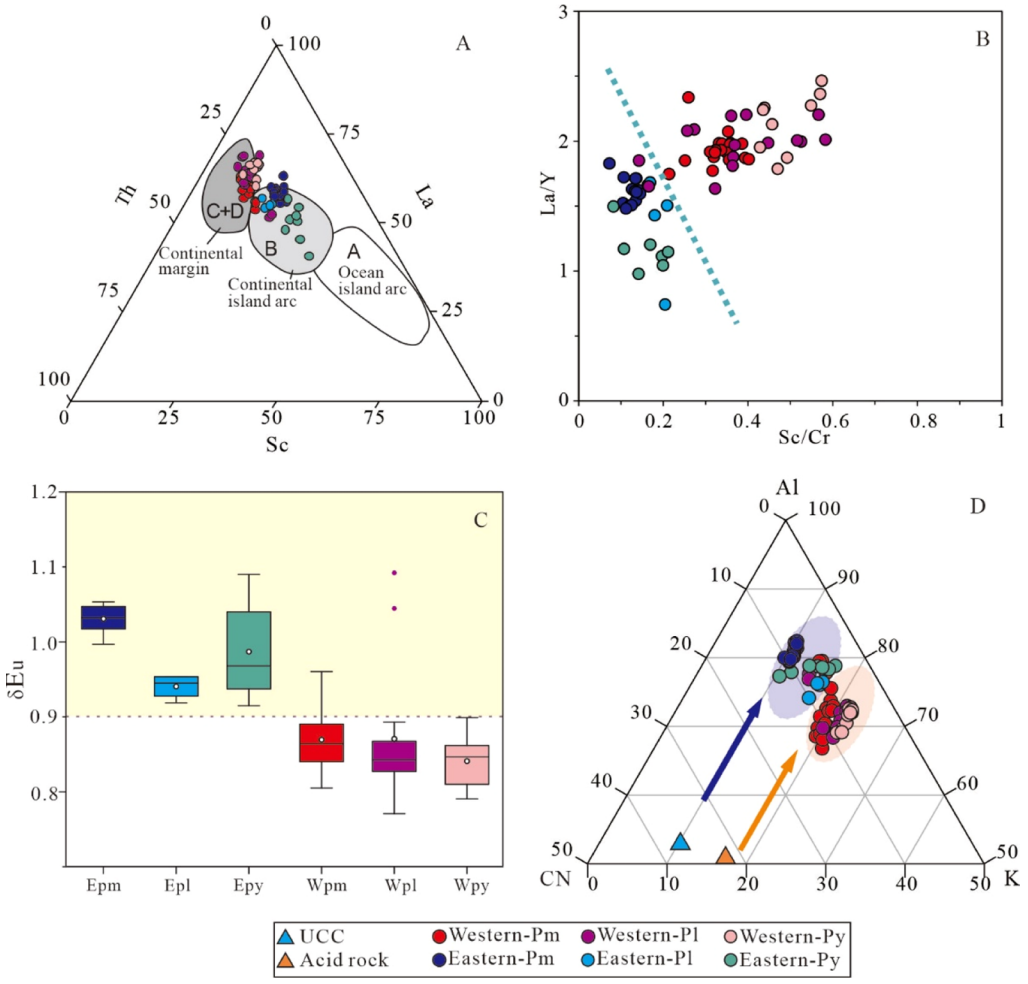

Figure 6. Element discrimination plots illustrating the sedimentary provenance and features of mudrocks in the Paleocene Lishui Sag[24,25] (modified from Roser and Korsch, 1988; Bhatia and Crook, 1986).

the abundance and source of OM in source rocks. PC and RC values are used to further discuss the composition of various OMs (Figure 5 and Table 2).

The TOC of each formation is obviously different (Figure 5A). In the WSS, the TOC of the Py Formation is the highest, with an average of 2.01%, and the TOC of the Pm Formation is the lowest, with an average of 1.27%. The abundances of the various formations' TOC values in the ESS are generally low, among which the TOC of the Py Formation is the highest, with an average of 1.18%; the TOC of the Pm Formation is the second highest at 1.06%; and the TOC of the Pl Formation is the lowest, with an average TOC value of only 0.69%. This means that the abundance of OM in the source rocks of each stratum in the ESS is significantly lower than that in the WSS.

Although the kerogen types of all the members in the sag are type III (Figure 5B,C), which is shown by the HI and OI indices, the thin-section observations show that the sources of these OMs in kerogen are not identical, thus we combine this with the variation in the HI index. Further comparison shows that the HI of the formations in the WSS is lower than that in the ESS. This result indicates that the source rocks in the WSS are more enriched in OM with low-HI characteristics. This type of OM is mainly input from terrigenous sources, such as higher plants. Such OM fragments can often be found in the source rocks in the WSS, which confirms the high content of externally input OM in the source rocks. The HI value of each formation in the ESS is generally higher, which manifests that during the depositional period in the Paleocene, the OM was more autochthonous. Combined with the observation results under the microscope, it can be found that the laminated OM is in the source rock, which is consistent with the morphological characteristics of the microbial mat OM.[21] This confirms that more autochthonous OM was generated in the water column during the depositional period in the ESS.

The differences in the abundance and source of OM in the WSS and ESS also result in the differences of PC and RC values. The TOC of each interval in the WSS is generally higher than that in the ESS, thus the PC and RC values are higher in the WSS too (Figure 5D). Further comparison of PC and RC characteristics of the two regions shows that the differences of PC between the WSS and ESS are relatively small, whereas the differences of RC are relatively large. Based on the above analysis, the different provenance of the OMs in the two subsags may be the main reason for the difference in RC. The rich terrestrial input OM in the WSS resulted in a higher proportion of RC, whereas the abundance of autochthonous OM in the ESS resulted in a relatively low proportion of RC.

In general, the OM in the ESS is mainly autochthonous, and the abundance is lower. The OM in the WSS is mostly input from terrigenous sources, but the abundance is generally higher than that in the ESS. Usually, the abundance of OM in source

https://doi.org/10.1021/acsomega.1c05764
ACS Omega 2022, 7, 5791−5803

rocks tends to increase with the increase of the autochthonous components,[3] but the opposite phenomenon appears in the Lishui Sag. The reasons for the differences in the abundance and types of OM need to be further analyzed in combination with environmental and provenance characteristics.

5.2. Tectonic Background and Parent Rock Characteristics. In this study, the La−Th−Sc, Sc/Cr−La/Y chart, and Eu anomalies were selected to reflect the differences in the tectonic background and provenance in each area. As the results of provenance analysis in the La−Th−Sc chart show (Figure 6A), the provenances of the ESS and WSS are significantly different. The abundances of the three elements, La, Th, and Sc in each formation of the ESS are mainly concentrated in zone B, indicating that the provenance of the rocks in the sedimentary period was mainly from the continental island arc and the rocks under this tectonic background are often mixed with upper crust-type parent rocks. The samples of each formation in the WSS are mainly concentrated in zone C + D, elucidating that the provenance of the sedimentary period was mainly from the continental margin, and this type of rock is often more likely to be mixed with acidic magmatic rock. The Sc/Cr−La/Y chart also indicates the distinct differences in elemental composition (tectonic background) between the WSS and ESS (Figure 6B).

After NASC standardization, we conducted an Eu anomaly analysis (Figure 6C) and found that the anomalous Eu values in the ESS and WSS are significantly different: among the formations in the WSS, the δEu value of the Pm Formation is the highest, with an average of 0.87, and the δEu values of the Pl and Py Formations are similar at 0.77 and 0.79, respectively. The average δEu value of the Pm Formation in the ESS is 1.02, followed by the δEu value of the Py Formation, with an average of 0.98, and the Pl Formation is the lowest, with an average of 0.94. Comparing the anomalous Eu values of the ESS and WSS, it can be found that the provenances of the two subsags are very different. The δEu values of more than 85% of the source rocks in the WSS are lower than 0.9, showing obvious negative anomalies, whereas those of the ESS are higher than 0.9. This result indicates that the rocks in the WSS are mixed with more acidic rock components, whereas the rocks in the ESS may be mixed with more intermediate and basic parent rocks. The provenance characteristics of the ESS and WSS shown by anomalous Eu values are consistent with the results of the La−Th−Sc chart.

The tectonic background and provenance characteristics of the eastern and western Lishui Sag affect the mineral composition of the source rocks. The major elements of the source rocks can reflect the mineral composition. The A−CN−K [Al_2O_3−(CaO* + Na_2O)−K_2O] chart can indicate the elemental composition of the weathering products of different parent rocks.[22,23] Based on this, we can further analyze the differences in the composition of silicate minerals in the source rocks of the ESS and WSS (Figure 6D). In this study, each index of the A−CN−K chart uses the molar percentage of oxide, where CaO* refers to the content of Ca in silicate. The correction of Ca is based on the correction method established by McLennan (1993): when CaO < Na_2O in the sample, CaO*=CaO and when CaO > Na_2O, then CaO*=Na_2O. By plotting the obtained data (Figure 6D), we find that the source rocks in the WSS are generally rich in K_2O and are consistent with the weathering products of the acidic magmatic rocks in the eastern part of the South China continent. This is the same result as the provenance revealed above. The rocks in the WSS are mixed with more acidic magmatic rocks, resulting in the relative enrichment of potassium-rich minerals, such as potassium feldspar and illite, after undergoing chemical weathering and deposition. The source rocks in each formation in the ESS are rich in Al_2O_3, which is consistent with the characteristics of weathering products in the upper crust. This indicates that more upper crust-derived rocks are mixed into the parent rock, resulting in less potassium-rich minerals in the source rocks formed by sedimentation than in the WSS. Therefore, we can conclude that the difference in provenance affects the composition of silicate minerals in the eastern and western parts of the study area.

According to the above analysis of geochemical elemental data and combined with previous research results, it can be determined that the Minzhe Uplift was strongly influenced by volcanic activity in the Cretaceous and developed a large set of acidic volcanic rocks. The WSS is adjacent to this uplift, and the source of the Paleocene mainly came from the acidic magmatic rocks in this uplift zone. The ESS is closer to the open sea, so during the Paleocene depositional period, more sedimentary rocks and intermediate and basic rock components were mixed into the rocks. Due to the barrier of the Lingfeng Rise, there was relatively less input of acidic igneous rocks from the Minzhe Uplift.[18,19]

5.3. Sedimentary Environment and Paleoproductivity Characteristics. *5.3.1. Selection of the Environmental and Paleoproductivity Index.* The redox environment and salinity are important factors affecting the source rock formation and OM enrichment. Therefore, this study focused on the redox conditions and salinity characteristics of the water column during the depositional period through geochemical elemental indicators.

Many elements are redox-sensitive elements, of which V, Ni, and U are important and effective indicators of redox conditions.[26] However, because V and Ni are significantly affected by diagenetic evolution, they may not be suitable for representing the sedimentary environment.[27] U element is more likely to be enriched in sediments under low oxygen reduction conditions and can be enriched by co-precipitation with OM in the deposition process, which can be seen as a typical redox-sensitive element.[7,28] Moreover, U element can be used as the "barometer" of redox conditions: U element and OM abundance will show a good correlation under the reducing conditions and no obvious correlation under the oxidizing conditions. Based on this, element U is selected as an indicator reflecting the redox conditions of rock deposition period. Al is believed to be a terrestrial element and rather stable after sedimentation, so the concentrations of U were normalized to Al before application to correct the dilution by OM and authigenic minerals.[7,29,30] In addition, the widely used Sr/Ba ratio is selected to reflect water salinity.

Paleoproductivity is an important indicator of the degree of OM enrichment in the water column. Higher productivity indicates the mass production of autochthonous organisms in the water column, which is a necessary condition for the enrichment of OM during the deposition of source rocks. C, N, P, Fe, Si, Cu, Ni, Zn, Ba, Mo, U, and other elements can reflect the primary productivity of the water column.[26,31] However, elements such as C and N migrate in large amounts during the process of recycling and later diagenesis.[32] Cu, Ni, Fe, and Zn are susceptible to seawater oxidation−reduction and pH values and are unstable. Fe tends to be affected by many late diagenetic factors, such as carbonate dissolution and

https://doi.org/10.1021/acsomega.1c05764
ACS Omega 2022, 7, 5791−5803

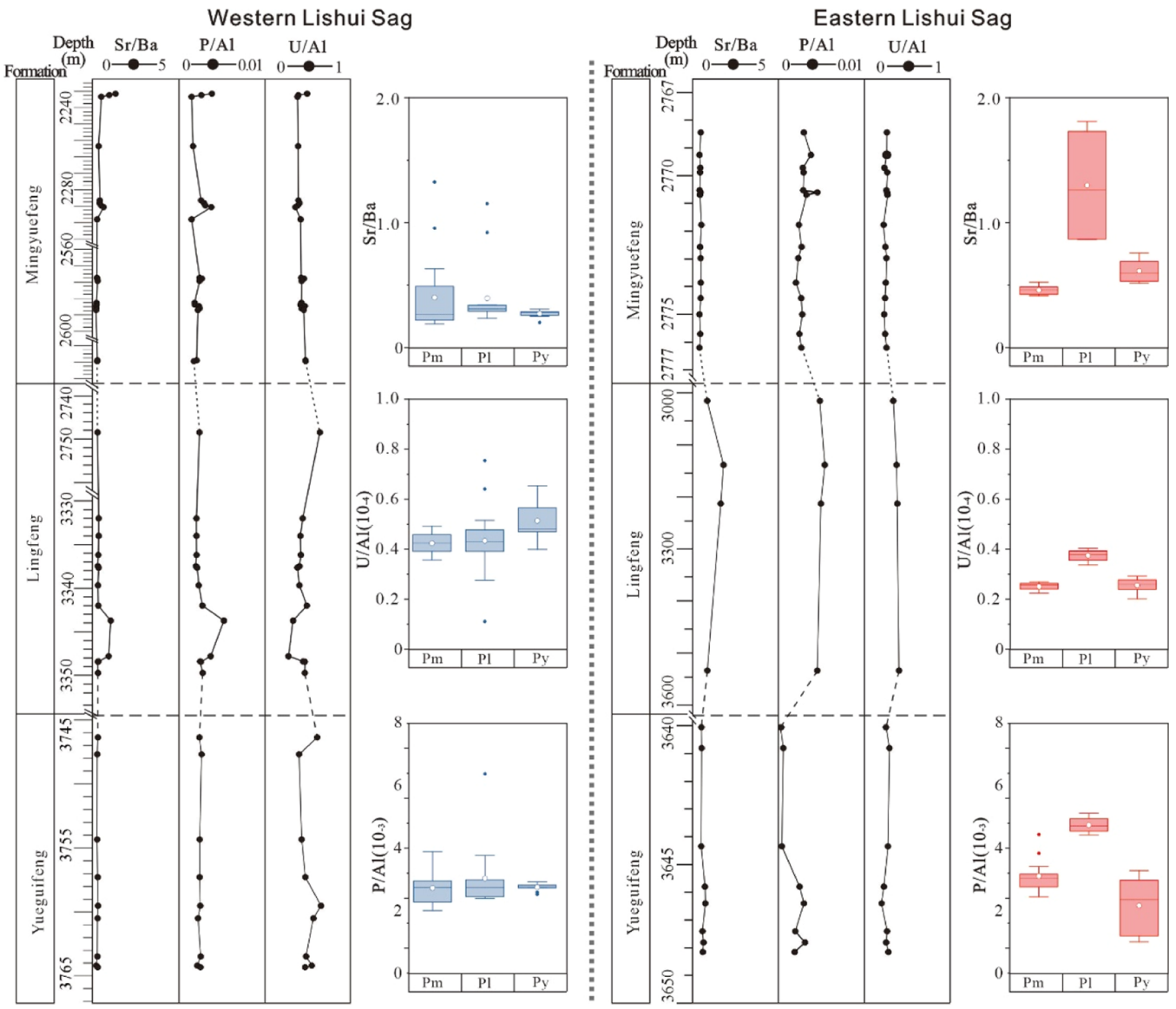

Figure 7. Environmental changes of each formation in the Lishui Sag.

recrystallization and metasomatism of elements. These elements above cannot be used as effective indicators of paleoproductivity. In addition, U, Mo, and Ba, as redox-sensitive elements, have difficulty restoring ancient productivity in an oxidizing environment. Therefore, this study selects P as a paleoproductivity indicator for analysis and uses the ratio of P and Al to reflect the relative enrichment of P to discuss the relative level of productivity in each formation.

5.3.2. Environmental Differences between the ESS and WSS. There are obvious differences in sedimentary environments between the ESS and the WSS (Figure 7). From the perspective of paleosalinity characteristics, the salinity of each formation in the ESS during the depositional period is significantly higher than that of the WSS, and it varies greatly. The average Sr/Ba ratio of the Pl Formation exceeds 1, which is significantly higher than that of the other two formations, indicating that the salinity of this formation during the sedimentary period was closer to that of seawater. The Sr/Ba ratio of each formation in the WSS is similar, generally lower than 0.5, reflecting the low and relatively stable salinity conditions of each interval.

The U/Al ratio can indicate the redox conditions. The U/Al ratio of each interval in the ESS is generally lower than that in the WSS. The average U/Al ratio of the Pl Formation in the ESS is slightly higher than that of the Pm and Py Formations, indicating that this formation was more reductive than the other two formations during the depositional period. The U/Al values of the intervals in the WSS are similar, reflecting the overall reduction in the intervals in the west relative to the east.

The paleoproductivity of each formation in the eastern and western parts of the study area during the depositional period is also different. The paleoproductivity of each formation in the ESS has changed greatly. From the depositional period of the Py Formation to the Pm Formation, the paleoproductivity experienced a change from low to high and then to low. Among them, the paleoproductivity of the Pl Formation is the highest and that of the Py Formation is the lowest. Compared with the ESS, the paleoproductivity of the formations in the WSS have very small variations. Except for the Py Formation, which is slightly higher than that of the eastern region, the paleoproductivity of the other two formations is lower than that of the ESS.

https://doi.org/10.1021/acsomega.1c05764
ACS Omega 2022, 7, 5791−5803

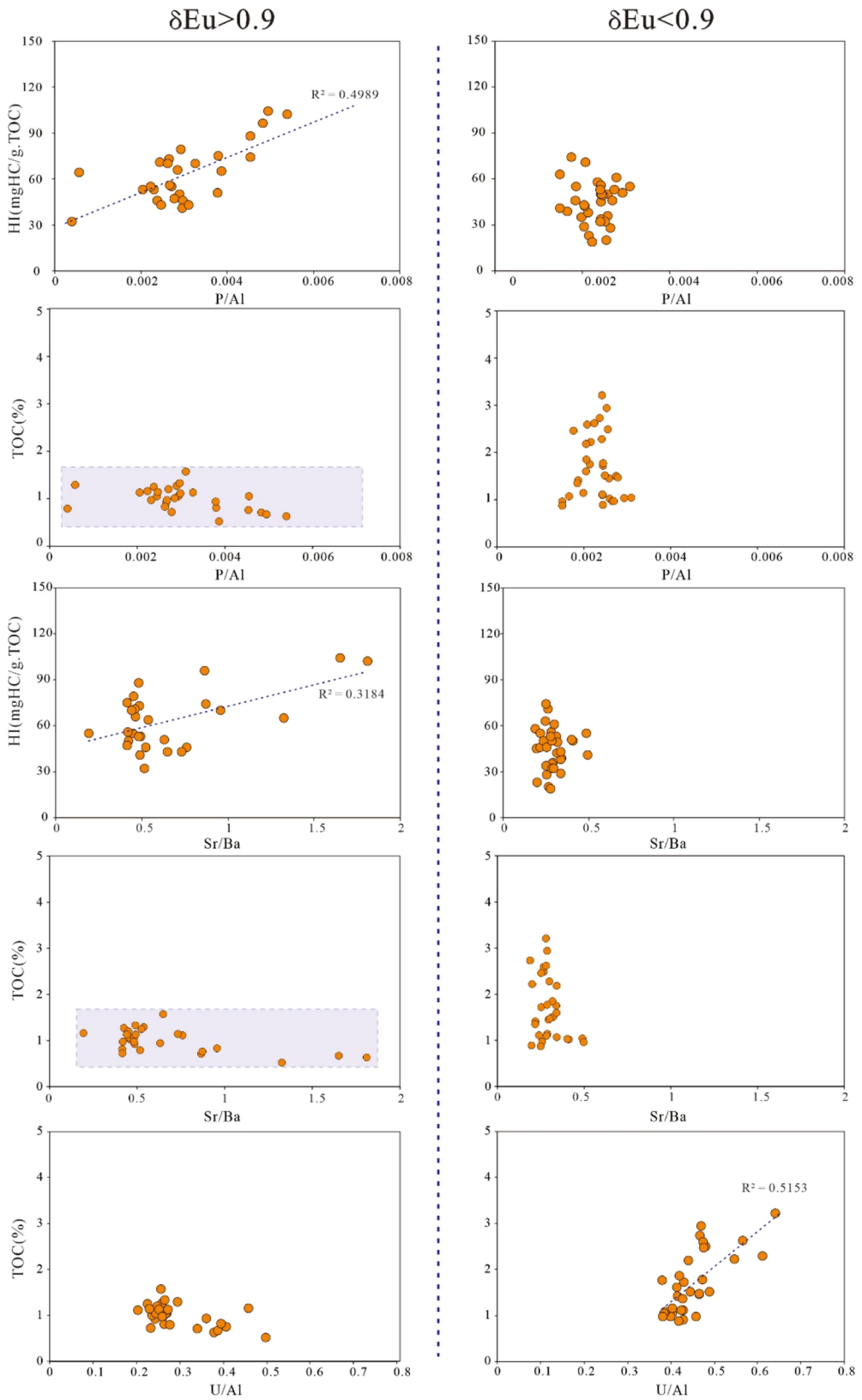

Figure 8. Correlation between environmental indicators and the type and abundance of OM.

The analysis results show that the environmental characteristics of the eastern and western formations are very different. The eastern region was a water environment that had high salinity, high productivity, and was oxidized, whereas the water environment of the western region had low salinity, low productivity, and was reductive. Differences in the sedimentary environment may have a certain impact on the formation of source rocks and the type and enrichment of OM.

5.4. Influence of Provenance and the Depositional Environment on the Enrichment of OM. According to

https://doi.org/10.1021/acsomega.1c05764
ACS Omega 2022, 7, 5791−5803

previous research results, the OM characteristics, provenance, and sedimentary environment of the ESS and WSS are significantly different. How the provenance and sedimentary environment affect the characteristics of OM deserves further study. As mentioned above, the Eu anomalies of the source rocks in the ESS and WSS are obviously different. The δEu values of the source rocks in the ESS are generally greater than 0.9, whereas those in the WSS are generally lower than 0.9. To more accurately discuss the influence of provenance and the environment on OM, this study uses a δEu value of 0.9 as the boundary and considers samples whose values are less than 0.9 to be the rocks that are more affected by the Minzhe Uplift and mixed with more acidic magmatic rocks. The samples whose values are larger than 0.9 indicate that the rocks contain more sedimentary rocks and other types of rocks. On this basis, we try to further analyze the relationship between the sedimentary environment of different provenance characteristics and the type and abundance of OM (Figure 8).

This study finds that for the source rocks whose provenance is offshore sediments, the changes in the salinity and paleoproductivity indicators of the sedimentary environment are relatively large, and salinity and paleoproductivity show a good positive correlation with the HI. With increasing salinity and paleoproductivity, the proportion of autochthonous OM in the water column continues to increase. The correlation of environmental indicators and TOC shows that the latter always fluctuates by approximately 1%, with obvious changes in the environment. This result indicates that environmental factors do not significantly affect the abundance of OM in rocks. Therefore, we believe that this is a "fake correlation", and these two environmental factors have little effect on the TOC. In summary, for this type of source rock, the salinity and paleoproductivity of the water column during the depositional process mainly controlled the type of OM within them. Previous studies have also found that, on the one hand, higher salinity at the bottom of the water column is a favorable condition for the preservation of OM.[5,33−36] On the other hand, the invasion of seawater is also an important reason for the increase in salinity, which also causes changes in the OM of the water column and an increase in paleoproductivity.[9] Generally, the increase in authigenic components of the water column and the increase in paleoproductivity are inevitably accompanied by an increase in the abundance of OM, but for this kind of rock, this phenomenon does not appear. We further compare the correlation between elemental U and TOC and find that there is no obvious correlation between them. Previous studies have determined that the redox conditions of water depend on the "barometer" in U's geochemical behavior: under reducing conditions, U deposition is closely related to OM, so the content of U is positively correlated with TOC, whereas under oxidizing conditions, this relationship does not exist.[7,37] Therefore, we can conclude that this kind of rock was in an oxidizing environment during the depositional period, which is the main reason that U/Al ratio and TOC are not correlated, and this environment is not conducive to the preservation of OM. Although the OM of this type of rock contains more autochthonous components from the water column, it tends to be oil-prone, and the oxidized depositional environment makes it difficult to preserve.

For rocks formed under the influence of the Minzhe Uplift, the salinity and paleoproductivity of the sedimentary environment are at a relatively low level, and there is no obvious positive correlation between salinity and paleoproductivity and the HI and TOC. This indicates that under this provenance condition, the salinity and paleoproductivity are generally low and have little change. The stable environment had no influence on the source of OM during the depositional period, which was mainly input OM from external sources, and the abundance of OM was not affected by the environment. This means that the salinity and productivity of the water column did not affect the OM characteristics of source rocks. However, the U/Al ratio in the WSS shows a good positive correlation with TOC. According to the previous discussion, the rocks were in a reducing environment.

In general, the source rocks with richer parent rock types produce good OM types during deposition, but due to the poor preservation conditions, the abundance of OM is usually low. The source rocks enriched in acidic igneous components do not have suitable environmental conditions for the large-scale formation of oil-prone OM. However, due to the better preservation conditions, the OM can be better preserved.

Combining the provenance and environmental characteristics of the east and west, it can be further determined that the ESS was close to the open sea during the Paleocene and was significantly influenced by sedimentary rocks and other provenances. The salinity and productivity of the water column were high, so source rocks with high-quality OM formed, but due to poor preservation conditions, the abundance of OM in source rocks was very low. The source rocks of the WSS were less affected by the open sea during deposition in the Paleocene, and the salinity and productivity of the water column were at a low level. The OM contained more allochthonous components, but the area was in a reducing environment. These OM types can be better preserved, resulting in a higher abundance.

5.5. Comparison of the Characteristics of the Source Rocks in the ESS and WSS and Exploration Strategies. Based on the analyses of elemental geochemistry and pyrolysis, it can be determined that there are obvious differences in the tectonic background, sedimentary environment, and OM characteristics of source rocks in the ESS and WSS. During the depositional periods of the Py, Pl, and Pm Formations, the tectonic environment of the WSS was relatively stable. The source rocks were formed in the continental marginal sedimentary belt and were near the source area. The OM was mainly input from terrigenous sources, and the water environment was relatively stable, with low salinity and productivity. However, due to the reductive water environment, the OM was preserved well and enriched.

The ESS was relatively far from the provenance during the Paleocene sedimentary period, and the environmental variation in the three formations was relatively large. In general, the salinity and paleoproductivity of the water in the ESS were higher than those in the WSS. This resulted in a relatively high content of autochthonous OM in the source rock, and the OM generally has high HI values. Nevertheless, due to the overall oxidation of the water column, the abundance of OM is relatively low.

In actual exploration, full consideration should be given to the large differences in the formation environment and OM characteristics of the source rocks in the ESS and WSS. Although the OM in the WSS was well preserved during the depositional period, the quality was poor, and its parent rocks have many high-carbon terrigenous components. Traditional kerogen theory believes that temperature is the decisive factor for OM to generate hydrocarbons.[38] Only high temperature

https://doi.org/10.1021/acsomega.1c05764
ACS Omega 2022, 7, 5791−5803

can promote the cracking of the poor OM types to generate hydrocarbons. Therefore, attention should be given to the tectonic characteristics of the working area, focusing on finding intervals that were deeply buried, developed at high levels, affected by deep and large faults, or had hydrothermal fluid input. Abnormally high temperatures promote hydrocarbon generation from source rocks in these formations.

The kerogen of the source rocks in the ESS mainly came from autochthonous OM in the water column. Although the oxygen-rich environment during the depositional period was not conducive to the preservation of OM, the HI of kerogen was still relatively high. For this kind of hydrogen-rich OM, its relationship with minerals is often very close,[17,39] and hydrocarbons can be generated at lower temperatures. Therefore, in the exploration of the ESS, to obtain source rocks that have sufficient hydrocarbon-generating capacity, we should focus on the area where the source rocks have a higher abundance of OM. Compared with the WSS, attention should be given to the area where the source rocks are more shallowly buried and have a relatively low degree of evolution.

As a result, due to the differences in the formation and provenance of source rocks in the ESS and WSS, different strategies should be adopted in future exploration.

6. CONCLUSIONS

This paper comprehensively analyzes the provenance and environmental characteristics of the Lishui Sag and their influence on the features of OM in the source rocks. The following conclusions can be drawn.

In the Paleocene, the formation of the source rocks in the ESS of the Lishui Sag was mainly affected by the input of offshore sedimentary rocks and other parent rocks. During the depositional process, as the salinity and paleoproductivity of the water column increased, the proportion of autochthonous OM in the water column continued to increase. However, due to the oxidizing environment, the abundance of OM was low.

The formation of the source rocks in the WSS was more affected by the acidic magmatic rocks of the Minzhe Uplift. The OM in the source rock was rich in terrigenous input components, and the sedimentary environment had little impact on the type of OM. However, due to the reducing environment, the OM was better preserved and had a higher abundance.

Due to the influence of provenance and the sedimentary environment, the source rocks formed in different areas of the sag have various characteristics; therefore, different exploration strategies need to be adopted. Attention should be given more to the source rocks of early-middle evolution stages in the exploration of the ESS, whereas in the WSS, the focus should be on the area where the source rocks have higher maturity.

■ ASSOCIATED CONTENT

Supporting Information

The Supporting Information is available free of charge at https://pubs.acs.org/doi/10.1021/acsomega.1c05764.

Pyrolysis data of wells and formations in the Lishui Sag (XLSX)

■ AUTHOR INFORMATION

Corresponding Authors

Xiang Zeng − *State Key Laboratory of Marine Geology, Tongji University, Shanghai 200092, China; Center for Marine Resources, Tongji University, Shanghai 200091, China*; Phone: +86-021-6598-8829; Email: 2013zengxiang@tongji.edu.cn

Jingong Cai − *State Key Laboratory of Marine Geology, Tongji University, Shanghai 200092, China; Center for Marine Resources, Tongji University, Shanghai 200091, China*; Email: jgcai@tongji.edu.cn

Authors

Luyao Zhang − *State Key Laboratory of Marine Geology, Tongji University, Shanghai 200092, China; Center for Marine Resources, Tongji University, Shanghai 200091, China*; orcid.org/0000-0001-8585-6980

Weilin Zhu − *State Key Laboratory of Marine Geology, Tongji University, Shanghai 200092, China; Center for Marine Resources, Tongji University, Shanghai 200091, China*

Lingcong Yuan − *State Key Laboratory of Marine Geology, Tongji University, Shanghai 200092, China; Center for Marine Resources, Tongji University, Shanghai 200091, China*

Complete contact information is available at: https://pubs.acs.org/10.1021/acsomega.1c05764

Notes

The authors declare no competing financial interest.

■ ACKNOWLEDGMENTS

This work was financially supported by the National Natural Science Foundation of China (NSFC) (41972126) and the National Natural Science Foundation of China (NSFC) (92055203).

■ REFERENCES

(1) Deng, Q.; Wang, H.; Wei, Z.; Li, S.; Zhang, H.; Liu, H.; Lekan Faboya, O.; Cheng, B.; Liao, Z. Different accumulation mechanisms of organic matter in Cambrian sedimentary successions in the western and northeastern margins of the Tarim Basin, NW China. *J. Asian Earth Sci.* **2021**, *207*, 104660.

(2) Li, D.; Li, R.; Zhu, Z.; Wu, X.; Cheng, J.; Liu, F.; Zhao, B. Origin of organic matter and paleo-sedimentary environment reconstruction of the Triassic oil shale in Tongchuan City, southern Ordos Basin (China). *Fuel* **2017**, *208*, 223−235.

(3) Tyson, R. V. *Sedimentary Organic Matter: Organic Facies and Palynofacies*; Academic Press: Berlin/Heidelberg, 1995; pp 431−462.

(4) Hou, L.; Ma, W.; Luo, X.; Tao, S.; Guan, P.; Liu, J. Chemical structure changes of lacustrine type-II kerogen under semi-open pyrolysis as investigated by solid-state 13C NMR and FT-IR spectroscopy. *Mar. Pet. Geol.* **2020**, *116*, 104348.

(5) Liu, B.; Song, Y.; Zhu, K.; Su, P.; Ye, X.; Zhao, W. Mineralogy and element geochemistry of salinized lacustrine organic-rich shale in the Middle Permian Santanghu Basin: Implications for paleoenvironment, provenance, tectonic setting and shale oil potential. *Mar. Pet. Geol.* **2020**, *120*, 104569.

(6) Cowie, G. L.; Hedges, J. I. The role of anoxia in organic matter preservation in coastal sediments: relative stabilities of the major biochemicals under oxic and anoxic depositional conditions. *Org. Geochem.* **1992**, *19*, 229−234.

(7) McManus, J.; Berelson, W. M.; Klinkhammer, G. P.; Hammond, D. E.; Holm, C. Authigenic uranium: Relationship to oxygen penetration depth and organic carbon rain. *Geochim. Cosmochim. Acta* **2005**, *69*, 95−108.

(8) Shu, Y.; Lu, Y.; Hu, Q.; Wang, C.; Wang, Q. Geochemical, petrographic and reservoir characteristics of the transgressive systems tract of lower Silurian black shale in Jiaoshiba area, southwest China. *Mar. Pet. Geol.* **2021**, *129*, 105014.

(9) Bohacs, K. M.; Carroll, A. R.; Neal, J. E.; Mankiewicz, P. J. Lake-basin type, source potential, and hydrocarbon character: an integrated sequence-stratigraphic-geochemical framework (in Lake basins through space and time). *AAPG Stud. Geol.* **2000**, *46*, 3−34.
(10) Liu, B.; Bechtel, A.; Sachsenhofer, R. F.; Gross, D.; Gratzer, R.; Chen, X. Depositional environment of oil shale within the second member of Permian Lucaogou Formation in the Santanghu Basin, Northwest China. *Int. J. Coal Geol.* **2017**, *175*, 10−25.
(11) Wei, H.; Chen, D.; Wang, J.; Yu, H.; Tucker, M. E. Organic accumulation in the lower Chihsia Formation (Middle Permian). of South China: Constraints from pyrite morphology and multiple geochemical proxies. *Palaeogeogr., Palaeoclimatol., Palaeoecol.* **2012**, *353*−*355*, 73−86.
(12) Bhatia, M. R. Rare earth element geochemistry of Australian Paleozoic graywackes and mudrocks: provenance and tectonic control. *Sediment. Geol.* **1985**, *45*, 97−113.
(13) LaMaskin, T. A.; Dorsey, R. J.; Vervoort, J. D. Tectonic controls on mudrock geochemisry, Mesozoic rocks of eastern Oregon and western Idaho, USA: Implications for cordilleran tectonics. *J. Sediment. Res.* **2008**, *78*, 765−783.
(14) Su, A.; Chen, H.; Cao, L.; Lei, M.; Wang, C.; Liu, Y.; Li, P. Genesis, source and charging of oil and gas in Lishui sag, East China Sea Basin. *Pet. Explor. Dev.* **2014**, *41*, 574−584.
(15) Li, Y.; Zhang, J.; Liu, Y.; Shen, W.; Chang, X.; Sun, Z.; Xu, G. Organic geochemistry, distribution and hydrocarbon potential of source rocks in the Paleocene, Lishui Sag, East China Sea Shelf Basin. *Mar. Pet. Geol.* **2019**, *107*, 382−396.
(16) Lei, C.; Yin, S.; Ye, J.; Wu, J.; Wang, Z.; Gao, B. Characteristics and deposition models of the paleocene source rocks in the Lishui Sag, East China Sea Shelf Basin: Evidences from organic and inorganic geochemistry. *J. Pet. Sci. Eng.* **2021**, *200*, 108342.
(17) Zhu, X.; Cai, J.; Wang, G.; Song, M. Role of organo-clay composites in hydrocarbon generation of shale. *Int. J. Coal Geol.* **2018**, *192*, 83−90.
(18) Chen, C.; Kai, Z.; Zhu, W.; Xu, D.; Wang, J.; Zhang, B. Provenance of sediments and its effects on reservoir physical properties in Lishui Sag, East China Sea Shelf Basin. *Oil Gas Geol.* **2017**, *38*, 963−972.
(19) Fu, X.; Zhu, W.; Chen, C.; Zhong, K.; Xu, C. Detrital zircon provenance of upper mingyuefeng formation in west slope of Lishui-Jiaojiang Sag, the East China Sea. *J. Earth Sci.* **2015**, *40*, 1987−2001.
(20) Shen, W.; Qi, B. Definition and distribution prediction of effective source rocks in Lishui Sag, East China Sea Basin. *Bull. Geol. Sci. Technol.* **2020**, *39*, 77−88.
(21) Schieber, J.; Bose, P. K.; Eriksson, P.; Banerjee, S.; Sarkar, S.; Altermann, W.; Catuneanu, O. *Atlas of Microbial Mat Features Preserved Within the Siliciclastic Rock Record*; Academic Press: Amsterdam, 2007; pp 242−245.
(22) McLennan, S. M. Weathering and global denudation. *J. Geol.* **1993**, *101*, 295−303.
(23) Nesbitt, H. W.; Young, G. M.; McLennan, S. M.; Keays, R. R. Effects of chemical weathering and sorting on the petrogenesis of siliciclastic sediments, with implications for provenance studies. *J. Geol.* **1996**, *104*, 525−542.
(24) Roser, B. P.; Korsch, R. J. Provenance signatures of sandstone-mudstone suites determined using discriminant function analysis of major-element data. *Chem. Geol.* **1988**, *67*, 119−139.
(25) Bhatia, M. R.; Crook, K. A. W. Trace element characteristics of graywackes and tectonic setting discrimination of sedimentary basins. *Contrib. Mineral. Petrol.* **1986**, *92*, 181−193.
(26) Algeo, T. J.; Maynard, J. B. Trace-element behavior and redox facies in core shales of Upper Pennsylvanian Kansas-type cyclothems. *Chem. Geol.* **2004**, *206*, 289−318.
(27) Qiao, J. Q.; Liu, L. F.; Shang, X. Q.; Yi, L. B. The relationship between V, Ni or V/Ni ration and each of organic matter abundance and diagenetic evolution stages in shales: taking the shales in Fukang Sag of Junggar Basin for example. *Bull. Mineral., Petrol. Geochem.* **2016**, *35*, 756−768.
(28) Tribovillard, N.; Algeo, T. J.; Baudin, F.; Riboulleau, A. Analysis of marine environmental conditions based onmolybdenum−uranium covariation—Applications to Mesozoic paleoceanography. *Chem. Geol.* **2012**, *324*−*325*, 46−58.
(29) Murray, R. W.; Leinen, M.; Isern, A. R. Biogenic flux of Al to sediment in the central equatorial Pacific Ocean: Evidence for increased productivity during glacial periods. *Paleoceanography* **1993**, *8*, 651−670.
(30) Xiong, Z.; Li, T.; Algeo, T.; Nan, Q.; Zhai, B.; Lu, B. Paleoproductivity and paleoredox conditions during late Pleistocene accumulation of laminated diatom mats in the tropical West Pacific. *Chem. Geol.* **2012**, *334*, 77−91.
(31) Brumsack, H.-J. The trace metal content of recent organic carbon-rich sediments: Implications for Cretaceous black shale formation. *Palaeogeogr., Palaeoclimatol., Palaeoecol.* **2006**, *232*, 344−361.
(32) Wan, X.; Liu, W.; Li, G.; Li, Y. Cretaceous black shale and dissolved oxygen content—A case study in southern Tibet. *Chin. Geol.* **2003**, *1*, 36−47.
(33) Crump, B. C.; Hopkinson, C. S.; Sogin, M. L.; Hobbie, J. E. Microbial biogeography along an Estuarine salinity gradient: Combined influences of bacterial growth and residence time. *Appl. Environ. Microbiol.* **2004**, *70*, 1494.
(34) Jiang, H.; Dong, H.; Yu, B.; Liu, X.; Li, Y.; Ji, S.; Zhang, C. L. Microbial response to salinity change in Lake Chaka, a hypersaline lake on Tibetan plateau. *Environ. Microbiol.* **2007**, *9*, 2603−2621.
(35) Taylor, R.; Fletcher, R. L.; Raven, J. A. Preliminary studies on the growth of selected 'Green Tide' algae in laboratory culture: Effects of irradiance, temperature, salinity and nutrients on growth rate. *Bot. Mar.* **2001**, *44*, 327−336.
(36) Zhang, Y.; Xi, B.; Xu, Q. Research on the possibility of using salinity as entrophication criteria indicator of saline lakes. *J. Environ. Eng. Technol.* **2011**, *1*, 260−263.
(37) Tribovillard, N.; Algeo, T. J.; Lyons, T.; Riboulleau, A. Trace metals as paleoredox and paleoproductivity proxies: an update. *Chem. Geol.* **2006**, *232*, 12−32.
(38) Tissot, B. P.; Welte, D. H. *Petroleum Formation and Occurrence*; Academic Press: Berlin/Heidelberg, 1984; pp 495−547.
(39) Cai, J.; Zhu, X.; Zhang, J.; Song, M.; Wang, Y. Heterogeneities of organic matter and its occurrence forms in mudrocks: Evidence from comparisons of palynofacies. *Mar. Pet. Geol.* **2020**, *111*, 21−32.

https://doi.org/10.1021/acsomega.1c05764
ACS Omega 2022, 7, 5791−5803